ISSN 0003-701X, Applied Solar Energy, 2024, Vol. 60, No. 2, pp. 255–266. © Allerton Press, Inc., 2024.

SOLAR INSTALLATIONS AND THEIR APPLICATION

Optimizing the Solar Photovoltaic Performance under Orthogonal Progressive Shading with Various Reconfigurations

Navneet[a], *, Neha Khurana[a], and Smita Pareek[b]

[a] *UIET/Maharshi Dayanand University, Rohtak, India*

[b] *Department of Electrical Engineering/BKBIET, Pilani, India*

**e-mail: navneety2@gmail.com*

Received August 6, 2023; revised November 26, 2023; accepted March 13, 2024

Abstract—Renewable energy is in very much demand in current time due to its many favorable environment effect. Solar energy is one of the frontline sources of renewable energy. Solar photovoltaic converts the solar light into electricity. The performance of the solar photovoltaic depends on various parameters and one of such parameters is shading behavior. Further, the shading pattern and the progress of the shading are also important for predicting the solar performance. The interconnections of solar cells also impact the performance of solar photovoltaic. Therefore, a 4 × 4 module with various interconnections such as series-parallel (SP), total cross tied (TCT), bridge-link (BL), honeycomb (HC) and triple tied (TT) are studied under the row and column wise shading pattern. Shading pattern on a 4 × 4 module is increased cell by cell in horizontal direction, both from left to right and right to left. In the similar fashion, the shading pattern is varied from top to bottom or vice-versa in vertical direction. This shading pattern progresses from first row to the last and first column to last column in a progressive fashion. The power-voltage and current-voltage characteristics of solar photovoltaic are investigated for the mentioned shading patterns using various reconfigurations. The power output is identical when all cells in a row or column are shaded. On the other hand, if only few cells are shaded on row or column then the power output with TCT connection is highest among all connections. Further, the power output is for complete column shading is much higher than complete row shading for all the connections. The theoretical simulated results can ensure better implementation of interconnection in hardware set-up based on the shading pattern.

Keywords: cell, partial shading, solar photovoltaic, series, series-parallel (SP), BL (bridge link), HC (honeycomb), total cross tied (TCT), and triple tied (TT)

DOI: 10.3103/S0003701X23601205

INTRODUCTION

Electricity can be produced from either fossil fuel or renewable source. The power generated out of fossil fuel is also termed as non-renewable energy sources (such as thermal power and nuclear power). Further, the fossil power has some limitations like storage of coal, global warming, radioactive waste, harmful effect on environment and so on. Nuclear power requires a lot of capital expenditure and installation and commissioning time for nuclear plant is few years. Moreover, the radioactivity waste disposal is another major concern. Therefore, renewable energy is in demand in current time [1]. One of the most preferred renewable energy sources is solar energy. It does not have any adverse effect on environment and requires low maintenance. The direct conversion of solar radiation into electricity is described as a solar photovoltaic (SPV) energy conversion as it is based on the photovoltaic effect. Solar cell is the basic unit of the solar photovoltaic system and the power produced by a single cell is not sufficient to meet power requirement cells for general purpose. Therefore, cells are connected by various interconnections to form modules and further array for increased power requirement. Solar photovoltaic system converts sunlight into electrical energy [2, 3]. The installation of solar photovoltaic system in India and worldwide is increasing year on year. But the efficiency of the energy produced from the solar photovoltaic is quite low and it is affected by various atmospheric conditions. Therefore, a lot of efforts are required to improve the performance of these solar photovoltaic. Solar photovoltaic performance is affected by many parameters such as temperature [4], dust and dirt [5–7], soil [8] and air mass effect [9]. The solar photovoltaic power output is most affected by solar irradiance variation [10, 11] due to partial shading condition. The source of this partial shading could be unpredictable flying bird, bird residue, dark cloud, neighboring building, tree etc. and some other sources [12]. Further, solar farms consist of PV modules are installed in multiple rows/columns and it is very much like to have shading of one panel

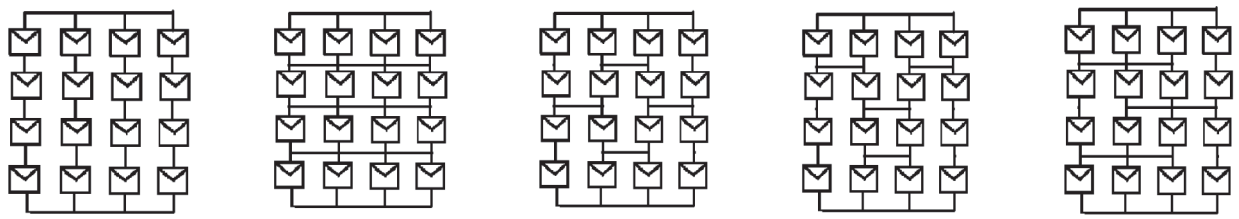

Fig. 1. Pictorial representation of solar cells Interconnection considered in the present study.

due to other during some particular time (h) [13]. However, this shading depends on the multiple parameters such as row spacing, row dimension, module tilt, inclination of land and the location. This partial shading behavior is one of the main barriers to its growth for solar photovoltaic. Few cleaning techniques [14] are developed but still limited for commercial application.

The performance of the PV module under the partial shading can be improved by using bypass diode, but it will have additional cost associated with it and complexity of creating multiple peaks in power-voltage characteristic curve. Although various maximum power point tracking (MPPT) techniques [15–17] exist to mitigate the partial shading effect on photovoltaic array. But this is quite challenging for the PV operator to select the most suitable technique for applications. The selection of MPPT techniques for solar power plant is completely dependent on the requirements such as cost and simplicity, accuracy and tracking speed. Therefore, the other ways to improve the performance under the partial shading is reconfigurations/interconnection of the cells. Fig 1 represents the cells interconnections for SP, TCT, BL, HC, and TT configurations.

In Series-parallel (SP) configuration, cells are connected in series and then these series connected strings are connected in parallel. The total-cross-tied (TCT) configuration is obtained from SP configuration by connecting ties across each row of junctions and thus voltages across the ties are equal. In bridge linked (BL) configuration a bridge is formed by connecting two modules in series and two in parallel. The Honeycomb (HC) configuration is essentially a modification of the BL configuration, aiming to leverage the benefits of both the Total Cross Tied (TCT) and BL configurations. In triple tied is also similar to TCT but instead of tying complete row, only three cells are tied to eliminate some of redundant ties of TCT.

Few researchers have investigated some of the interconnection connections under few possible shading patterns. It observed [18] that the irradiance variation due to partial shading affects short circuit current more than open circuit voltage and exhibit a significant decrement. The effect of shading pattern on module is studied [19]. When the shadow on modules is moving either horizontally or vertically then both topologies, SP and TCT, can produce the same maximum power. TCT topology produces more power than SP in case of diagonal shadow pattern on module. But this investigation does not specify anything on the progressive nature of the shading pattern in either direction. The progressive nature of shading pattern is investigated in later study [20] on a 4 × 4 PV panel for SP, TCT and BL connections but it was limited to last row and first column. The shading is moving from one cell to another and then the complete row and column. SP interconnection gives more power and current than TCT interconnection when shadow progresses from left to right on lowest row of module. TCT interconnection gives more power and current when the shadow progresses lowest to highest row on leftmost column. The power output is same for all the topologies when leftmost column and bottom row is fully shaded. The different configurations mainly SP, TCT, BL and HC are compared [21] for the shading pattern either on bottom rows or lower triangular or lower quarter. If the bottom rows are shaded, then no effect of interconnections is observed. But lower triangular and lower quarter produce maximum power in TCT and SP connection respectively.

It is also investigated that the PV array performance for S, P, SP, TCT, BL and HC topologies [22, 23] with various shading patterns such as uneven row, uneven column, diagonal and random, short and narrow, short and wide, long and narrow and long and wide. It is observed that under uneven row shading pattern, BL topology generate the maximum power without bypass diode and TCT topology generate the maximum power with bypass diode, due to a greater number of cross ties in connection and minimized mismatch loss. The shading patterns investigated are either on the full row or column with same/variable solar irradiance. Therefore, a literature gap exists for progressive shadow pattern i.e., shadow moving on one module to another and then to complete column of an array.

It is studied that the various configuration mainly series/parallel connected [24] PV modules for its performance under partial shading conditions. Author further explained the use of bypass diode to improve the PV performance under partial shading condition.

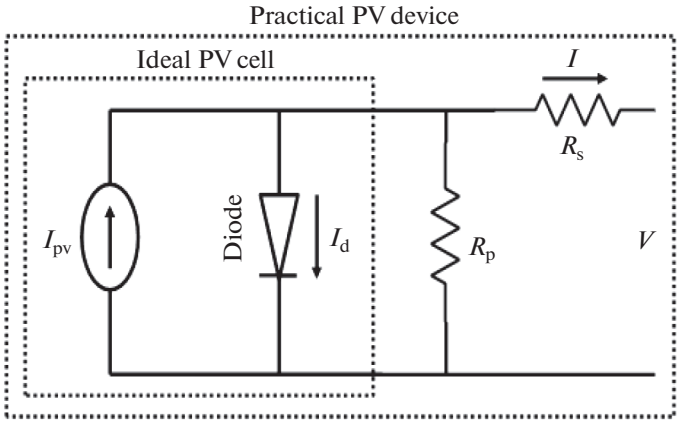

Fig. 2. Equivalent circuit of practical photovoltaic cell.

It is reported that reduction of power depends upon the shaded area, type of shade on module and configuration of photovoltaic module. Some recent investigations [25–28] on S, P, SP, TCT and BL configurations of PV array with various connections are investigated for some limited shading patterns which are row, column, diagonal, or L-shape etc. Logic based reconfigurations [29, 30] and hybrid configuration [31] are investigated for performance enhancement under partial shading but with limited shading pattern which can occur quite often. Hence the limited literature is available on progressive/moving shading pattern behavior for partial shading effect. This shading behavior is very common as sun motion keeps changing every moment and hence the shades on panel.

The progressive investigation of shading pattern is limited to either last row or first column with few topologies mainly SP, TCT and BL. Therefore, all the possible conventional interconnections mentioned in Fig 1 are investigated under the progressive shading pattern moving on complete module. Progressive shading for logic based re-configuration is not the scope of current research. Further, the progressive nature of the shading pattern is investigated for both direction i.e. the shading pattern moving on one cell to another either from left to right or right to left and similarly for top to bottom for column wise shading pattern.

METHODOLOGY

Modeling of Photovoltaic System

Open circuit voltage (V_{OC}), short circuit current (I_{SC}) and maximum power point (P_{max}) are the three basic important performance parameters of a solar PV cell. But for accurate model, some additional information may be required. The simplified equivalent circuit is a single diode model [20], shown in Fig. 2.

Solar photovoltaic cells generate current due to light (I_{pv}). This light current is linearly dependent on the solar irradiance and has the influence of temperature. I–V characteristic equation [32] for a single diode derived from the circuit diagram as:

$$I = I_{pv} - I_d - I_p. \quad (1)$$

Here, I_d = diode current, which is defined by Shockley diode equation as below:

$$I_d = I_0\left[\exp\frac{V + R_s I}{aV_t} - 1\right]. \quad (2)$$

I_{pv}, I_d, and I_p are substituted in the characteristic Eq. (1), which modifies as below:

$$I = \left(I_{pv} - I_0\left[\exp\left(\frac{(V + R_s I)}{aV_t}\right) - 1\right] - \frac{(V + R_s I)}{R_p}\right),$$

V is load voltage, I is current across the load; R_s and R_p are the equivalent series and parallel resistance of the array.

Photovoltaic current, I_{pv}, and the terminologies used in the formula are referred from Ahmed et al. [33], as stated below:

$$I_{PV} = [I_{STC} + \beta_I (T_{cell} - T_{STC})]\frac{H_t}{H_{STC}}. \quad (3)$$

Here I_{STC} is the light generated current at standard test condition (in A)

β_I is current coefficient (A/K);

T_{cell} is the actual temperature [K];

T_{STC} is cell's temperature at standard test condition [K];

H_t is the real solar radiation incident on the PV module [W/m^2] and H_{STC} is the irradiance of standard test condition [W/m^2].

A correlation for cell temperature is formed [34] as defined below, which is reliable for locations within a certain temperature and solar irradiance.

$$T_{cell} = T_\infty + 7.8\times10^{-2} H_t, \quad (4)$$

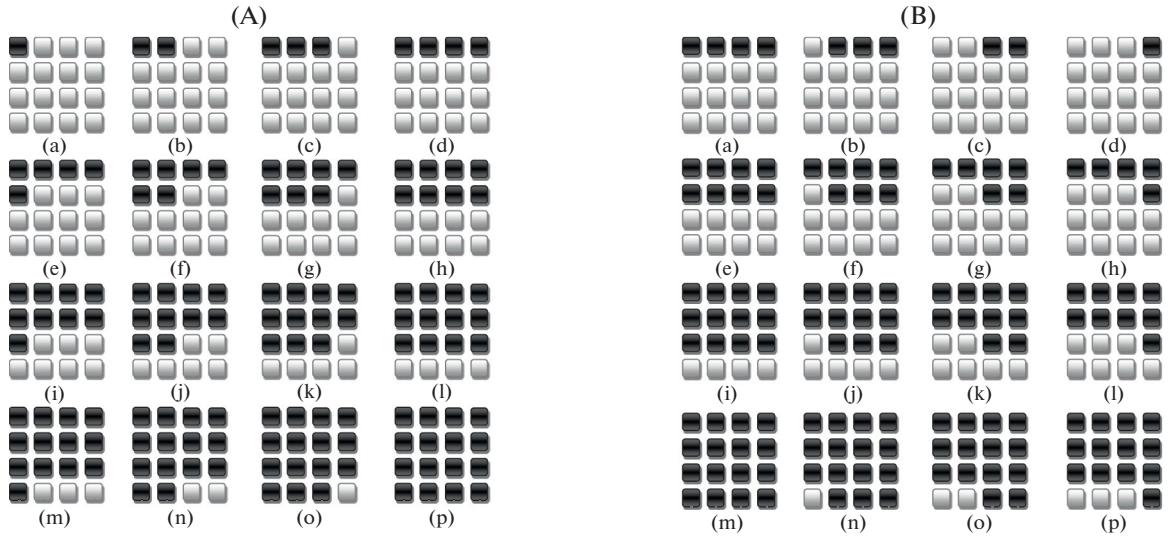

Fig. 3. Progresses of shading pattern in all rows: (A) Shading progression from left to right, (B) Shading progression from right to left.

where T_∞ is ambient air temperature and other parameters are explained earlier.

The study is performed in MATLAB Simulink simulation to access the PV performance. Five parameter Simulink model is considered for the evaluation. The cell characteristics of the five parameter model considered for the simulation in this study are stated below:

Apart from the cell characteristics, the manufacturing characteristics (such as mono-crystalline silicon (M–Si), polycrystalline silicon (P–Si), and amorphous silicon (A–Si)), play a significant role in defining PV efficiency. Another important parameter is temperature coefficient of I_{SC} and V_{OC} are also cell characteristic parameter. Default parameters from Matlab Simulink R2014a, for above mentioned parameters are considered. However, cell temperature and solar irradiance being the prime parameter for controlling the solar performance.

Assumption and Limitation

There are three models available in MATLAB Simulink to simulate the PV cell. Matlab Simulink model is simulated on computer with Intel(R) Core(TM) i5-9300HF CPU @ 2.40GHz. A 5-parameter model is considered for simulation in current study. This model considers simplifying assumptions to Eq. (1):

The impedance of the parallel resistor is infinite.

This model is parameterized in terms of short-circuit current and open-circuit voltage the block uses to derive these parameters.

Various Shading Patterns Considered for Investigation

A module of 4 × 4 PV cells is simulated for the various shading pattern. Numerous shading patterns on PV module are categorized into two groups. The shading pattern progresses from left to right or vice-versa and in another pattern progresses from top to bottom or vice-versa. Figures 3 and 4 illustrate the shading pattern variation cell by cell. Dark filled squares depict the shading on those cells (irradiations of 200 W/m^2) and other PV cell filled with light grey receives (irradiations of 1000 W/m^2). There could be various other shading patterns on a panel. Some of them had been already investigated by other researcher [18–22, 28] and by author [29, 35]. Therefore, author has focused only on the progressive shading pattern both in horizontal and vertical direction as scope for the current research as this study has not reported in the literature yet.

In Fig. 3A the shading progresses from one cell to another in a first row (a, b, c, d). Once all the cells in a first row are completely shaded and shading progresses on second row (e, f, g, h). Further the shading progresses on third row (i, j, k, l) and fourth row (m, n, o, p) of 4 x4 PV array in a similar fashion of first row. Figure 3B demonstrate the shading patterns similar to Fig. 3A which is just mentioned above, but the shading progresses from right to left instead of left to right. As mentioned above, the shading pattern is moved in a vertical fashion and the various shading patterns are demonstrated in Fig. 4.

RESULTS AND DISCUSSION

Short circuit current (I_{SC}), open circuit voltage (V_{OC}) and maximum power (P_{max}) are defined as the characteristic parameters of PV module, which are evaluated in the current research.

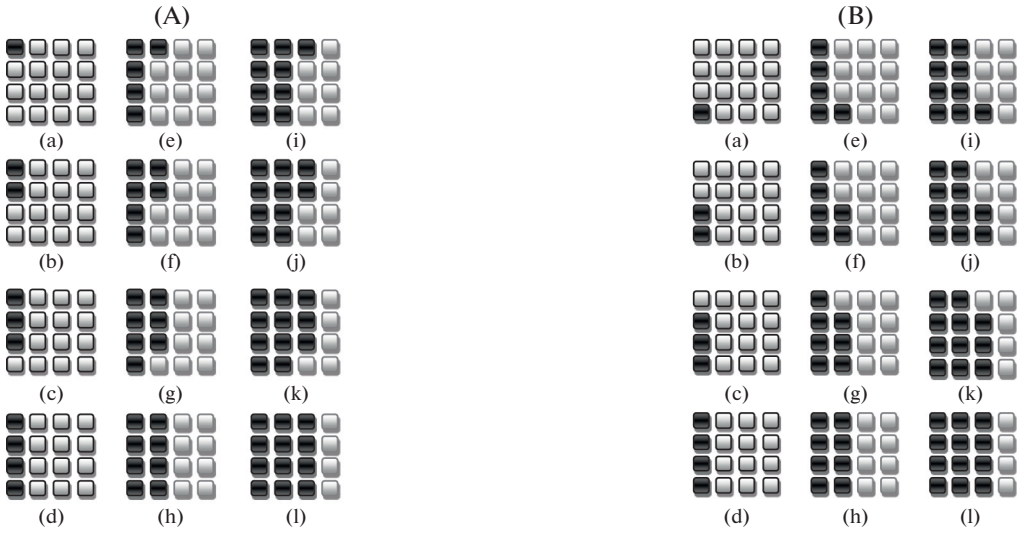

Fig. 4. Progresses of shading pattern in all columns: (A) Shading progression from top to bottom, (B) Shading progression from bottom to top.

When the first cell of first row or column in a 4 × 4 array is shaded then I_{SC}, V_{OC} and P_{max} is 23.49 A, 2.388 V and 43.69 W. The minimum power output is 43.69 W in SP connection and maximum is 47.5 W in TCT connection. This trend of minimum power output in SP connection and maximum in TCT connection is observed for most of the shading patterns except when the full row is shaded. The power produced by TT, HC and BL connection is always in-between TCT and SP connection. This pattern of maximum power output is also similar for progressive shading pattern from one cell to the complete column. As the shading further progress to full column or row then the maximum power output is identical for all topologies/interconnections which means TCT does not have any advantages over other topologies in case of full column shading.

Tables 2–5 list the performance parameter of a 4 × 4 solar PV array under different row wise shading patterns as mentioned in Fig. 3A.When the shading pattern progresses from right to left Fig. 3B, then the performance parameters are identical to left to right shading except for TT connection. Therefore, the performance parameters are not listed again in the tabular form so that redundant data or abundance of data can be avoided. The performance parameters in the tabular form both from top to bottom and bottom to top, as mentioned in Fig. 4, can be referred from the research [35].

The PV characteristic parameters are compared for shading patterns progressing from left-right and right-left. It has been observed that weather shading moves either from left to right or right to left, the PV characteristic parameters does not vary in all connection except TT connection.

The performance parameter listed in Table 2 is plotted for graphical representation. These graphs are plotted for Fig. 3A (a–d) shading pattern. As explained earlier and visible from Fig 5 through Fig. 10, TCT connection produces maximum power output when full row is not shaded. As the shadow moves on full row, then the power output is identical

Table 1. Cell characteristics parameter consider for simulation

Parameters	Values
Short-circuit current, I_{SC}	7.34 A
Open-circuit voltage, V_{OC}	0.6 V
Irradiance used for measurements, Ir_0 (H_{STC})	1000 W/m^2
Quality factor, N	1.5
Series resistance, R_s	0 Ohm
P_{max} (maximum power)	3.39 W
I_m (maximum current)	6.77 A
V_m (maximum voltage)	0.50 V

Table 2. Performance parameters for shading progressing from left to right on first row

Shaded region	Connections	I_{SC}, A	V_{OC}, V	I_m, A	V_m, V	P_{max}, W
Fig. 3A (a)	SP	23.5	2.4	21.8	2.0	43.7
	TCT	23.5	2.4	23.0	2.1	47.5
	BL	23.5	2.4	22.0	2.0	45.3
	HC	23.5	2.4	22.2	2.1	45.9
	TT	23.5	2.4	22.7	2.1	47.1
Fig. 3A (b)	SP	17.6	2.4	16.3	2.0	33.1
	TCT	17.6	2.4	17.3	2.1	36.7
	BL	17.6	2.4	17.1	2.1	35.8
	HC	17.6	2.4	16.5	2.1	34.2
	TT	17.6	2.4	17.0	2.1	36.0
Fig. 3A (c)	SP	11.7	2.4	10.9	2.1	22.5
	TCT	11.7	2.4	11.5	2.2	24.8
	BL	11.7	2.4	11.3	2.1	24.0
	HC	11.7	2.4	11.5	2.1	24.7
	TT	11.7	2.4	11.4	2.1	24.1
Fig. 3A (d)	SP	5.9	2.3	5.7	2.2	12.4
	TCT	5.9	2.3	5.7	2.2	12.4
	BL	5.9	2.3	5.7	2.2	12.4
	HC	5.9	2.3	5.7	2.2	12.4
	TT	5.9	2.3	5.7	2.2	12.4

Table 3. Performance parameters for shading progressing from left to right on second row

Shaded region	Connections	I_{SC}, A	V_{OC},V	I_m, A	V_m, V	P_{max}, W
Fig. 3A (e)	SP	5.9	2.3	5.6	2.1	11.9
	TCT	5.9	2.3	5.8	2.2	12.4
	BL	5.9	2.3	5.7	2.1	11.9
	HC	5.9	2.3	5.8	2.1	12.4
	TT	5.9	2.3	5.7	2.2	12.4
Fig. 3A (f)	SP	5.9	2.3	5.6	2.1	11.6
	TCT	5.9	2.3	5.7	2.1	12.3
	BL	5.9	2.3	5.7	2.1	11.9
	HC	5.9	2.3	5.7	2.1	11.6
	TT	5.9	2.3	5.7	2.1	12.2
Fig. 3A (g)	SP	5.9	2.3	5.6	2.0	11.5
	TCT	5.9	2.3	5.8	2.1	12.1
	BL	5.9	2.3	5.6	2.0	11.5
	HC	5.9	2.3	5.6	2.1	11.7
	TT	5.9	2.3	5.6	2.0	11.5
Fig. 3A (h)	SP	5.9	2.3	5.6	2.0	11.3
	TCT	5.9	2.3	5.6	2.0	11.3
	BL	5.9	2.3	5.6	2.0	11.3
	HC	5.9	2.3	5.6	2.0	11.3
	TT	5.9	2.3	5.6	2.0	11.3

Table 4. Performance parameters for shading progressing from left to right on third row

Shaded region	Connections	I_{SC}, A	V_{OC}, V	I_m, A	V_m, V	P_{max}, W
Fig. 3A (i)	SP	5.9	2.3	5.6	2.0	11.0
	TCT	5.9	2.3	5.6	2.0	11.3
	BL	5.9	2.3	5.6	2.0	11.3
	HC	5.9	2.3	5.5	2.0	11.0
	TT	5.9	2.3	5.5	2.0	10.9
Fig. 3A (j)	SP	5.9	2.2	5.5	1.9	10.7
	TCT	5.9	2.3	5.6	2.0	11.2
	BL	5.9	2.2	5.5	1.9	10.7
	HC	5.9	2.3	5.5	2.0	10.9
	TT	5.9	2.3	5.6	2.0	10.9
Fig. 3A (k)	SP	5.9	2.2	5.5	1.9	10.5
	TCT	5.9	2.2	5.7	2.0	11.0
	BL	5.9	2.2	5.5	1.9	10.7
	HC	5.9	2.2	5.5	1.9	10.5
	TT	5.9	2.2	5.6	1.9	10.9
Fig. 3A (l)	SP	5.9	2.2	5.5	1.9	10.4
	TCT	5.9	2.2	5.5	1.9	10.4
	BL	5.9	2.2	5.5	1.9	10.4
	HC	5.9	2.2	5.5	1.9	10.4
	TT	5.9	2.3	5.6	2.0	11.3

Table 5. Performance parameters for shading progressing from left to right on fourth row

Shaded region	Connections	I_{SC}, A	V_{OC}, V	I_m, A	V_m, V	P_{max}, W
Fig. 3A (m)	SP	5.9	2.2	5.5	1.8	10.1
	TCT	5.9	2.2	5.5	1.9	10.3
	BL	5.9	2.2	5.4	1.9	10.1
	HC	5.9	2.2	5.4	1.9	10.1
	TT	5.9	2.2	5.5	1.9	10.3
Fig. 3A (n)	SP	5.9	2.2	5.4	1.8	9.9
	TCT	5.9	2.2	5.5	1.9	10.2
	BL	5.9	2.2	5.4	1.9	10.0
	HC	5.9	2.2	5.4	1.8	10.0
	TT	5.9	2.2	5.5	1.9	10.2
Fig. 3A (o)	SP	5.9	2.2	5.4	1.8	9.7
	TCT	5.9	2.2	5.5	1.8	10.1
	BL	5.9	2.2	5.4	1.8	9.6
	HC	5.9	2.2	5.4	1.8	9.7
	TT	5.9	2.2	5.4	1.8	9.6
Fig. 3A (p)	SP	5.9	2.2	5.4	1.8	9.5
	TCT	5.9	2.2	5.4	1.8	9.5
	BL	5.9	2.2	5.4	1.8	9.5
	HC	5.9	2.2	5.4	1.8	9.5
	TT	5.9	2.2	5.4	1.8	9.5

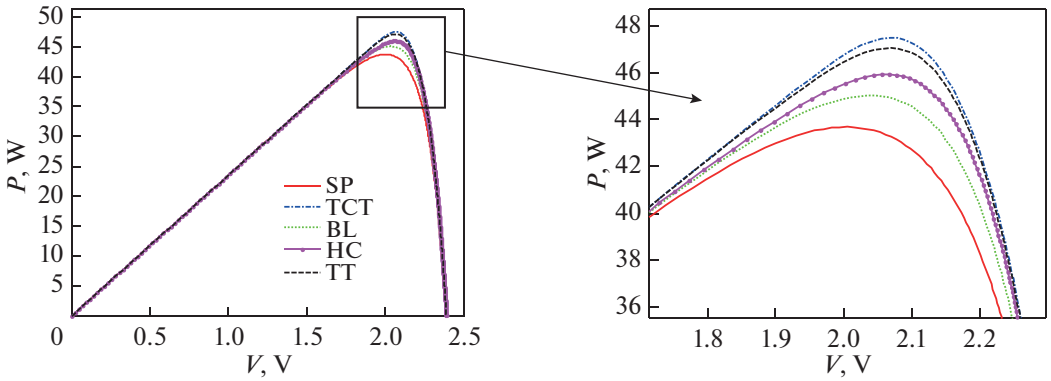

Fig. 5. PV Characteristics curve of 4 × 4 PV array for one cell shaded (refer Fig. 3A (a)) for all configurations.

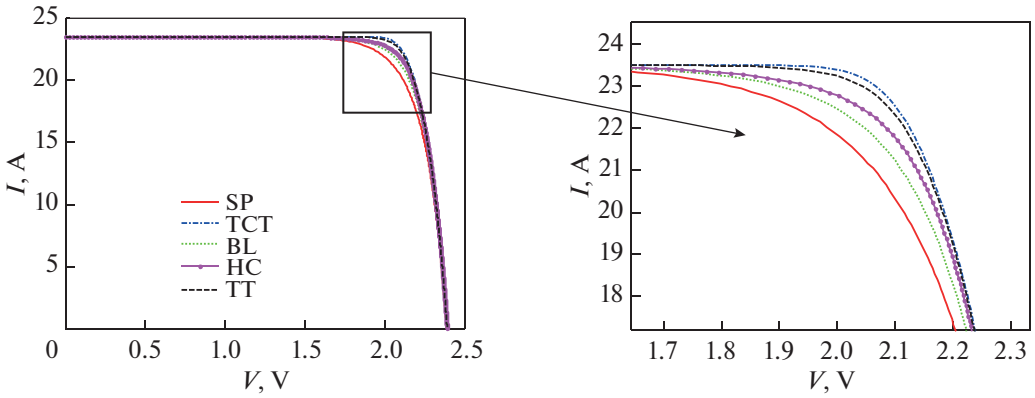

Fig. 6. IV Characteristics curve of 4 × 4 PV array for one cell shaded (refer Fig. 3A (a)) for all configurations.

for all connections. This can be referred from Fig. 11. Therefore, in case of full row shading, SP connection can be preferred solution because it is simpler and would be cost effective.

Row wise Shading pattern (Tables 2–5 and Figs. 5–11).

Maximum power varies from 12.44 to 47.5 W for various configurations, when the shading is on first row. If this shading progresses on second row, third row and forth row then maximum power varies from 11.34 to 12.38 W, 10.38 to 11.28 W, 9.522 to 10.32 W. Therefore, the maximum power mainly reduces when the shadow progresses in the first row. The open circuit voltage (V_{OC}) and short circuit current (I_{SC}) of a 4 × 4 PV array with various interconnection are ~2.300 V and 23.49 A respectively, when the shadow

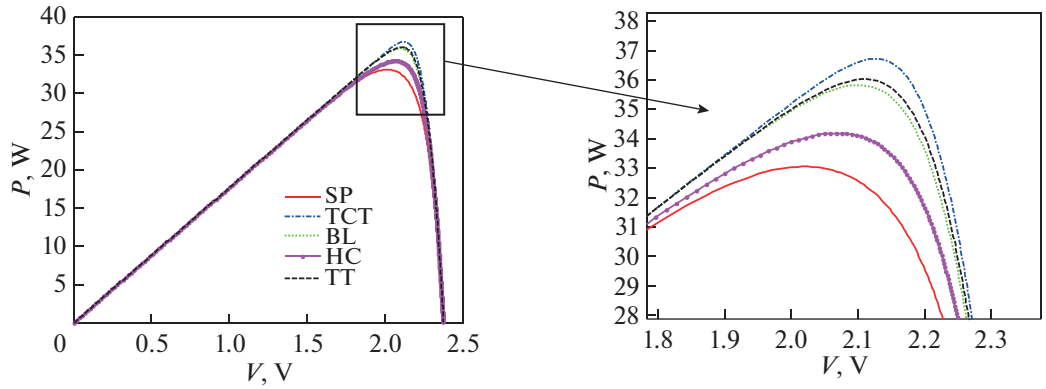

Fig. 7. PV Characteristics curve of 4 × 4 PV array for two cells shaded (refer Fig. 3A (b)) for all configurations.

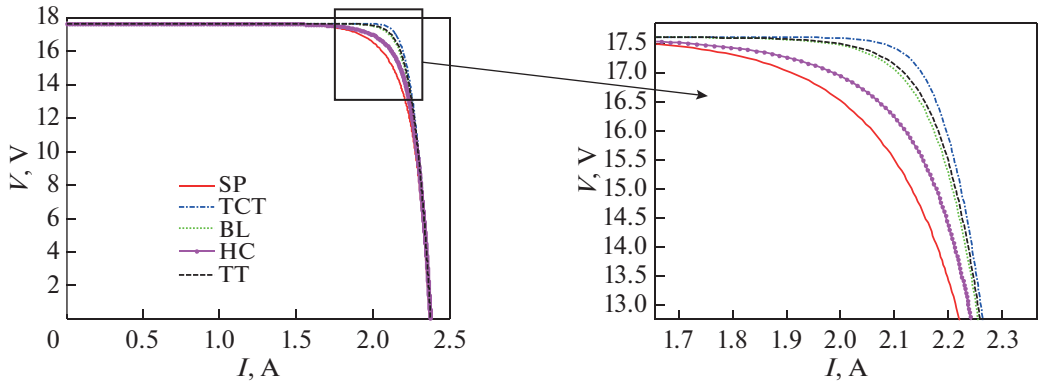

Fig. 8. IV Characteristics curve of 4 × 4 PV array for two cells shaded (refer Fig. 3A (b)) for all configurations.

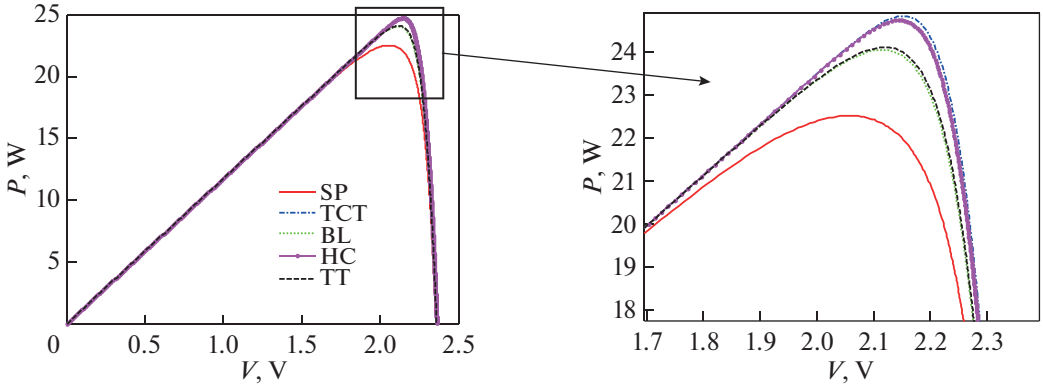

Fig. 9. PV Characteristics curve of 4 × 4 PV array for three cells shaded (refer Fig. 3A (c)) for all configurations.

progresses on first cell of first row. If this shadow pattern continues on second cell of first row in addition to first cell, then V_{OC} and I_{SC} are ~2.300 V and 17.620 A. If this shadow pattern continues on third cell of first row in addition to first two cells of first row, then V_{OC} and I_{SC} are ~2.300 V and 11.34 A respectively. Short circuit current (I_{SC}) further reduces to 5.872 A but open circuit voltage (V_{OC}) is same, when the shadow further moves on full row.

Column wise Shading pattern [29].

The results, both the tabular and graphical, for the same can be referred from [35]. When the first cell of first column is shaded which is identical to Fig. 3A (a). The power output as mentioned earlier is highest for

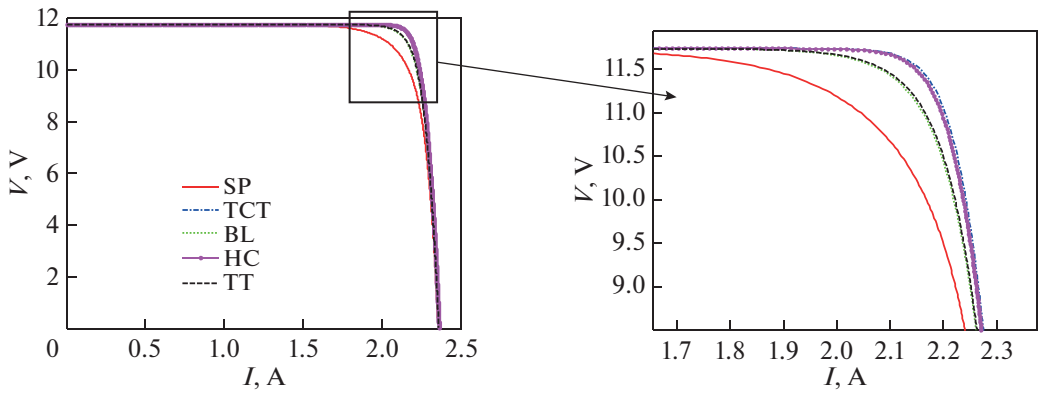

Fig. 10. IV Characteristics curve of 4 × 4 PV array for three cells shaded (refer Fig. 3A (c)) for all configurations.

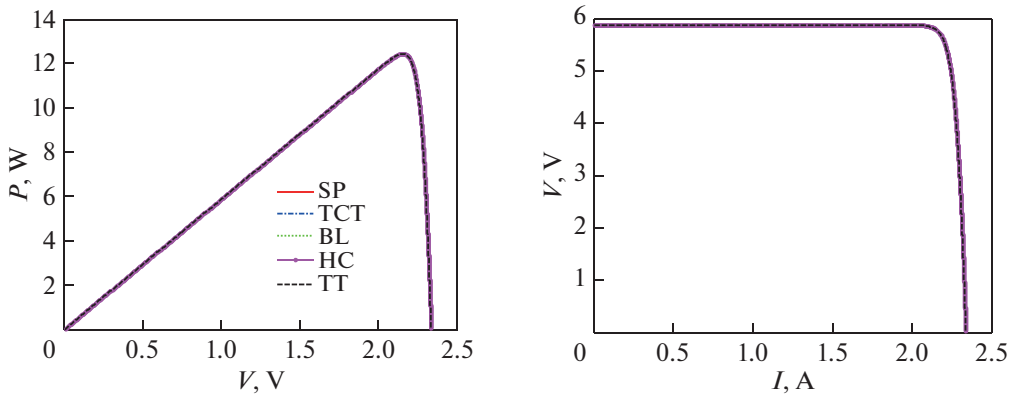

Fig. 11. IV and PV Characteristics curve of 4 × 4 PV array for full row shaded (refer Fig. 3A (d)) for all configurations.

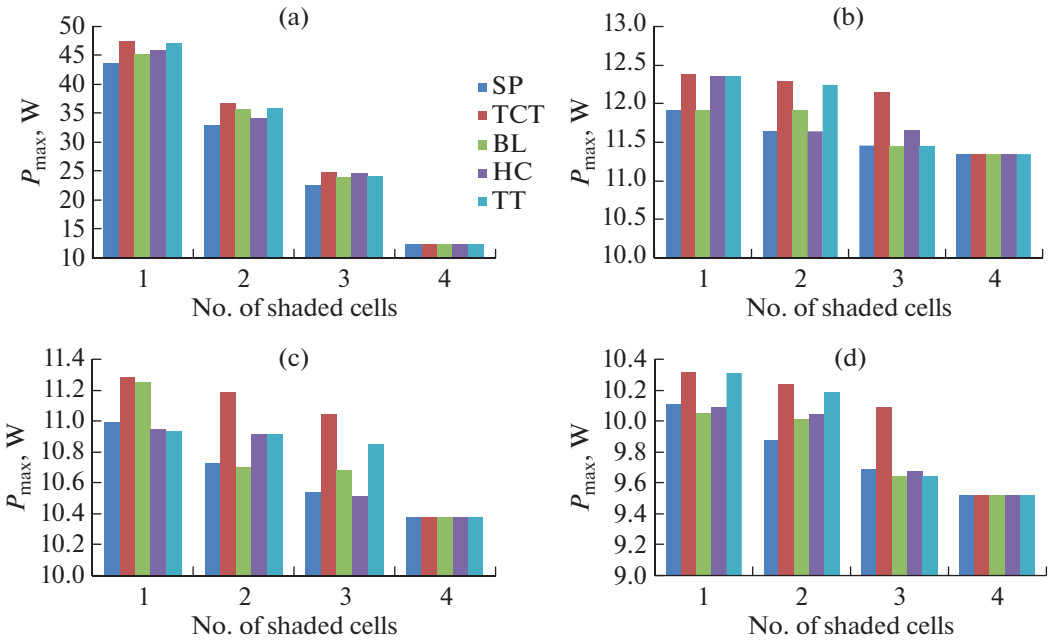

Fig. 12. Comparison of the maximum power among the reconfiguration for all rows (a) Shading progression on first row, (b) Shading progression on second row, (c) Shading progression on third row, (d) Shading progression on fourth row.

TCT connection, which is 47.500 W at 23.490 A, 2.391 V and least for SP connection i.e. 43.690 W at 23.490 A, 2.388 V. As the shading further progresses on the subsequent cells then the difference in power output for various connections reduces. Once, either the complete column or complete row is shaded then the power output is identical for the configurations.

Figures 12 and 13 explains the maximum power output for various topologies with progressive shading pattern on a complete row and complete column respectively. The horizontal axis denotes the number of shaded cells. Therefore, the number 1 on *x*-axis represents the first cell of a row is shaded that can be from left to right. Similarly, the no. 2 represents the shading on the next cell i.e. first two consecutive cells of a row are shaded from left to right. Furthermore, the no. 3 represent shading on first three consecutive cells from left to right. At last, no. 4 represent the complete row shaded. Therefore, the progressive nature of shading is investigated and plotted in Figs. 12 and 13. It is observed that if only few cells are shaded in a row/column and not the complete row then there is significant difference in maximum power output for various topologies. If this shading is on full row/column, then the maximum power output is identical for all the topologies. It is further observed that the power output in case of complete column shading is much higher than complete row shading. Therefore, vertical shading pattern is always desirable on a panel to maximize the power output.

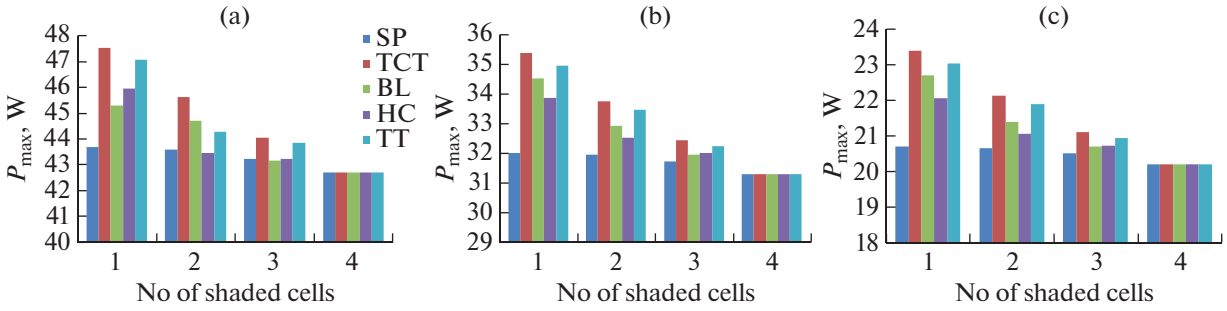

Fig. 13. Comparison of the maximum power among the reconfiguration for column shading pattern (a) Shading progression on first column, (b) Shading progression on second column, (c) Shading progression on third column.

Once the first row or column is fully shaded and shading moves on second and third subsequent row or column progressively, then the variation of maximum power output is similar to first row/column shading variation as shown in Figs. 12a, 13a but with a reduced magnitude due to large shaded area. Therefore, in case of full row shading, SP connection can be preferred solution because it is simpler and cost effective.

CONCLUSIONS

A 4 × 4 array for various configurations SP, TCT, BL, HC and TT is analyzed for their performance under various partial shading conditions both along horizontal (row) and vertical (column) direction. The progressive shading patterns for all the configurations are analyzed in detail. It is observed that power produced is dependent on partial shading pattern and number of shaded cells in a module. Further, the solar PV performance parameter is not influenced when the shading in a row moves either left-right or right-left (top to bottom and bottom to top in case of column shading) manner except TT configuration. Further, the variation in maximum power among various configurations is highest when the cells of first row/column are shaded. As this shadow progresses on complete row/column then the power output is identical for all configurations. Further, Column wise shading pattern produces more power than row wise shading pattern.

TCT connection performance is best among the selected configuration is the full row/column is not shaded, but in case of full row shading all connections produce same power. Therefore, SP connection can be preferred when the shadows progress on a full column because the connection is simpler and would be cost effective solution.

ACKNOWLEDGMENTS

I would like to acknowledge the UIET, MDU for providing the opportunity. Further, I would like to have a special note of acknowledgement for my husband who supported me in all ways.

FUNDING

This work is performed in Matlab Simulink on computer. The expense associated with hardware or software, to carry out this research is born by author for her doctoral research degree. There is not external or sponsorship for the carried work.

CONFLICT OF INTEREST

The authors of this work declare that they have no conflicts of interest.

REFERENCES

1. Elistratov, V.V., Renewable energy trends within the concept of low-carbon development, *Appl. Sol. Energy,* 2022, vol. 58, pp. 594–599.
2. Rahman, S., Green power: What is it and where can we find it?, *IEEE Power Energy Mag.,* 2003, vol. 1, no. 1, pp. 30–37.
3. Jager-Waldau, A., Photovoltaics and renewable energies in Europe, *Renewable Sustainable Energy Rev.,* 2007, vol. 11, no. 7, pp. 1414–1437.
4. Hasan, M.A. and Parida, S.K., Temperature dependency of partial shading effect and corresponding electrical characterization of PV panel, *IEEE Power Energy Society General Meeting, Denver, CO,* 2015.
5. Sulaiman, S.A., Singh, A.K., Mokhtar, M.M.M., and Bou-Rabee, M.A., Influence of dirt accumulation on performance of PV panels, in *International Conference on Technologies and Materials for Renewable Energy, Environment and Sustainability (TMREES14), Energy Procedia,* 2015, vol. 50, pp. 50–56.
6. Ketjoy, N. and Konyu, M., Study of dust effect on photovoltaic module for photovoltaic power plant, *Energy Procedia,* 2014, vol. 52, pp. 431–437.
7. Mejia, F., Kleissl, J., and Bosch, J.L., The effect of dust on solar photovoltaic systems, *Energy Procedia,* vol. 49, pp. 2370–2376, 2015.
8. Maghami, M.R., Hizam, H., Gomes, C., Radzi, M.A., Rezadad, M.I., and Hajighorbani, S., Power loss due to soiling on solar panel: A review, *Renewable Sustainable Energy Rev.,* 2016, vol. 59, pp. 1307–1316.

9. Riza, K.S., Al-Waeli, A.A.K., and Al-Asadi, K.A.H., The impact of air mass on photovoltaic panel performance, *Eng. Sci. Rep.,* 2016, vol. 1, no. 1.

10. Pareek, S., Runthala, R., and Dahiya, R., Mismatch losses in SPV systems subjected to partial shading conditions, in *International Conference on Advanced Electronic Systems (ICAES),* 2013, pp. 343–345.

11. Pareek, S. and Dahiya, R., Environmental effect consideration on photovoltaic module, in *Recent Trends in Energy, System and Control (RTESC-13),* 2013.

12. Ahmed, J. and Salam, Z., A critical evaluation on maximum power point tracking methods for partial shading in PV systems, *Renewable Sustainable Energy Rev.,* 2015, vol. 47, pp. 933–953.

13. Alsadi, S.Y. and Nassar, Y.F., A general expression for the shadow geometry for fixed mode horizontal, step-like structure and inclined solar fields, *Sol. Energy,* 2019, vol. 181, pp. 53–69.

14. Dyskin, V.G., Yuldoshev, I.A., and Shoguchkorov, S., Method for snow removal from the surface of a photovoltaic array, *Appl. Sol. Energy,* 2021, vol. 57, pp. 409–412.

15. Kurniawan, A. and Shintaku, E., A neural network-based rapid maximum power point tracking method for photovoltaic systems in partial shading conditions, *Appl. Sol. Energy,* 2020, vol. 56, no. 3, pp. 157–167.

16. Sellami, A., Kandoussi, K., Otmani, R.E., Eljouad, M., Mesbah, O., and Hajjaji, A., A novel auto-scaling MPPT algorithm based on perturb and observe method for photovoltaic modules under partial shading conditions, *Appl. Sol. Energy,* 2018, vol. 54, no. 3, pp. 149–158.

17. Ibrahim, A., Obukhov, S., and Aboelsaud, R., Determination of global maximum power point tracking of PV under partial shading using cuckoo search algorithm, *Appl. Sol. Energy,* 2019, vol. 55, no. 6, pp. 367–375.

18. Pareek, S. and Dahiya, R., Simulation and performance analysis of individual module to address partial shading cum parameter variation in large photovoltaic fields, *J. Energy Power Sources,* 2015, vol. 2, no. 3, pp. 99–104.

19. Pareek, S. and Dahiya, R., Output power comparison of TCT & SP topologies for easy-to-predict partial shadow on a 4 × 4 PV field, *Appl. Mech. Mater.,* 2014, vol. 612, pp. 71–76.

20. Pareek, S. and Dahiya, R., Power output maximization of partially shaded 4/4 PV field by altering its topology, *Energy Procedia,* 2014, vol. 54, pp. 116–126.

21. Sharma, M., Pareek, S., and Singh, K., Comparative study of different configuration techniques to address the outcome of partial shading conditions on solar photovoltaic system, *IOP Conf. Series: Mater. Sci. Eng.,* 2019, vol. 594, no. 1.

22. Pendem, S.R. and Mikkili, S., Modelling and performance assessment of PV array topologies under partial shading conditions to mitigate the mismatching power losses, *Sol. Energy,* 2018, vol. 160, pp. 303–321.

23. Desai, A.A. and Mikkili, S., Modelling and analysis of PV configurations (alternate TCT-BL, total cross tied, series, series parallel, bridge linked and honey comb) to extract maximum power under partial shading conditions, *CSEE J. Power Energy Syst.,* 2022, vol. 8, no. 6, pp. 1670–1683.

24. Mertia, P., Kothari, S., Agrawal, N., and Panwar, N.L., Experimental analysis of solar photovoltaic system under partial shading, *Int. J. Curr. Microbiol. Appl. Sci.,* 2020, vol. 9, pp. 1623–1630.

25. Mohamed, A.M., EI-Sayed, A.M., Mohamed, Y.S., and Ramadan, H.A., Enhancement of photovoltaic system performance based on different array topologies under partial shading conditions, *J. Adv. Eng. Trends,* 2021, vol. 40, no. 1, pp. 49–61.

26. Bingol, O. and Ozkaya, B., Analysis and comparison of different PV array configurations under partial shading conditions, *Sol. Energy,* 2018, vol. 160, pp. 336–343.

27. Bana, S. and Saini, R.P., Experimental investigation on power output of different photovoltaic array configurations under uniform and partial shading scenarios, *Sol. Energy,* 2017, vol. 127, pp. 438–453.

28. Yadav, K., Kumar, B., and Swaroop, D., Mitigation of mismatch power losses of PV array under partial shading condition using novel odd even configuration, *Energy Rep.,* 2020, vol. 6, pp. 427–437.

29. Navneet, Khurana, N., and Pareek, S., Performance comparison of solar photovoltaic array under partial shading conditions with puzzle based reconfigurations, *Appl. Sol. Energy,* 2022, vol. 58, no. 3, pp. 395–409.

30. Kurniawan, A. and Shintaku, E., A neural networkbased rapid maximum power point tracking method for photovoltaic systems in partial shading conditions, *Appl. Sol. Energy,* 2020, vol. 56, no. 3, pp. 157–167.

31. Jariri, N. and Aroudam, E., Novel hybrid photovoltaic array arrangement to mitigate partial shading effects, *Appl. Sol. Energy,* 2022, vol. 58, pp. 813–828.

32. Wikipedia. Theory of solar cells. https://en.wikipedia.org/wiki/Theory_of_solar_cells. Accessed June 29, 2021.

33. Hafez, A.A., Nassar, Y.F., Hammdan, M.I., and Alsadi, S.Y., Technical and economic feasibility of utility-scale solar energy conversion systems in Saudi Arabia, *Iran. J. Sci. Technol., Trans. Electr. Eng.,* 2019.

34. Nassar, Y. and Salem, A., The reliability of the photovoltaic utilization in southern cities of Libya, *J. Desalination,* 2017, vol. 209, pp. 86–90.

35. Navneet, Khurana, N., and Pareek, S., Addressing the partial shading effects on solar photovoltaic array by reconfiguration, *Int. J. Renewable Energy Technol.,* 2022, vol. 13, no. 2, pp. 178–195.

Publisher's Note. Allerton Press remains neutral with regard to jurisdictional claims in published maps and institutional affiliations.